NIPES

Advances in Engineering Design Technology

Journal homepage: www.nipesjournals.org.ng

# Design and Development of a Hand Operated Grinding Machine

***Erameh Andrew A[a] and Adingwupu Anthony C[b]***

[a,b]Department of Mechanical Engineering, College of Engineering, Igbinedion University, Okada, Edo State Nigeria

**ARTICLE INFORMATION**

*Article history*:
Received 28 February 2019
Revised 11 March 2019
Accepted 07 April 2019
Available online 8 April 2019

*Keywords*:
Grinding
Prime Mover
*Gear Assembly*
Abrasive grinding wheels

**ABSTRACT**

*Grinding food items is a very important part of food processing. This paper is focused on the design and fabrication of a manually operated domestic foodstuff grinding machine whose cost is affordable to the common man while ensuring durability, maintainability and reliability. The conventional prime mover is replaced with a hand operated geared assembly which will reduce the total cost of the assembly while maintaining the grinding quality and capacity of the machine. The results showed an average mass of residue from the constructed machine after drying to be 63g and with a finness of less than 500µm particle size, the overall percentage of the constructed machine was 75percent.*

## 1. Introduction

Grinding Machines are tools which employ abrasive grinding wheels to grind materials [1]. Grinding in our community is a necessity as most agricultural products require grinding as one of the food processing processes. For instance, to prepare a delicious meal, there is need to grind the ingredients such as melon, pepper, onions, etc. As such, man through the ages has devised various devices of breaking large amount of food substances into smaller bits for proper processing [2]. Among these devices is the antique domestic grinding stone. The conventional foodstuff grinding machine is operated with the aid of a prime mover which could be in form of an internal combustion engine or an electric motor [3]. Though, it is efficient but its cost of purchase has not made it a common machine in every home as it ought to be. Its high cost is usually borne by the prime mover component. In a bid to make it a household machine which will be affordable by all and sundry, a design is being sought after which replaces the prime mover with a hand operated geared assembly which will reduce the total cost of the assembly while maintaining the grinding quality and capacity of the machine. Grinding is one of the oldest manufacturing processes. Since the stone age grinding was used to sharpen the tools of man. Wooden arrows were sharpened by rubbing them on gravel. Later, softer stones were ground with relatively harder stones to obtain axes. Looking at the history of grinding, it is clear that the whole evolution of the grinding process is in line with the discovery of new and harder abrasives from gravel and sandstone via oxides such as diamonds and synthetic carbides [4].

By the discovery of synthetic abrasives such as silicon carbide, in the late nineteenth century, the development of the grinding process made a major breakthrough. From that period, the research on grinding developed because of the complexity of the whole process. One major difficulty which prompted research works was to get the actual profiles and to find the active cutting edges from the profiles [3].

## 2. Materials and Method

### 2.1 Working Principle

The modus operandi of the domestic grinding machine is abrasion [3]. The two grinding discs have slightly rough surfaces facing each other, packed into a housing which is mounted on the shaft by means of bearing. The produce which being fed through the hopper, is rolled by the worm thread on the shaft as the handle is turned. Each turn being made by the handle is amplified by the gear assembly which in turn translates to increased speed in the worm shaft. To obtain the required pastry, an adjustment bolt is screwed to the grinding disc end of the shaft; this help in adjusting the distance between the crushing disc surfaces.

### 2.2 Shaft Design

#### 2.2.1 Transmitted torque

A healthy human can sustain an average cranking speed of 50rpm [4]. Using the selected transmission ratio of 6:1 for the gears used, this translates to 300 rpm at the main shaft.
Angular velocity at this operational speed is:

$$\omega = \frac{2\pi n}{60} \tag{1}$$

$$\omega = \frac{(2)(\pi)(300)}{60} = 31.4 rad/sec.$$

Transmitted power in kWH) and angular velocity are related as:

$$H = M_t w \tag{2}$$

$$H = \frac{2\pi n M_t}{60} \tag{3}$$

And

$$M_t = \frac{9550H}{n} \tag{4}$$

$$M_t = \frac{(9550)(1.8)}{300} = 57.3Nm$$

Considering functional resistance at the bearings, an applicable coefficient of friction for steel on steel is μ= 0.2 [5] Hence power transmitted by the main shaft is

$$H = 1.2pr \tag{5}$$

$$H = (1.2)(1.5) = 1.8kW$$

Shaft Loading
Components are arranged on the main shaft as shown in Figure 1.

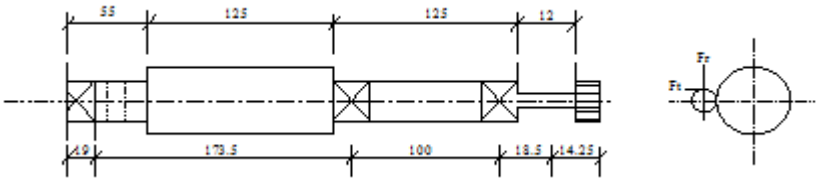


Figure 1: Arrangement of components on shaft

Loads acting on the shaft are indicated as in Figure 2.

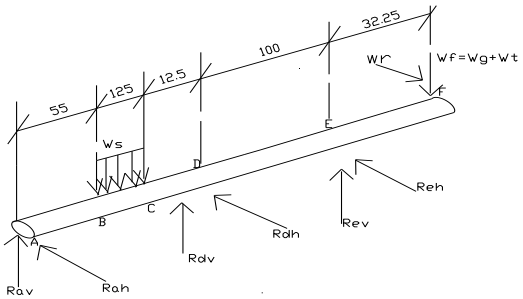


Figure.2: Load acting on shaft

The shaft is under vertical and horizontal loading as shown in Figure 3 and Figure 4 respectively when resolved.
Vertical loading

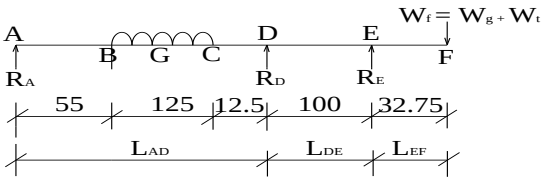


Figure.3: vertical loading

Horizontal loading

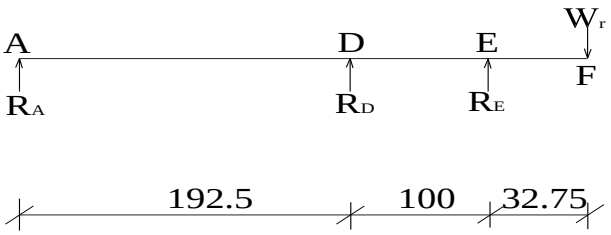


Figure.4: Horizontal loading

**Loads on the gear tooth.**
Tangential load on the gear tooth is

$$W_t = \frac{60{,}000H}{\pi Dn} \quad (6)$$

$$\frac{(60{,}000)(1.8)}{(\pi))(24)(300)} = 4.775kW$$

The radial load is obtained as

$$w_r = w_t tan\emptyset \quad (7)$$

$W_r = 4.775 \tan 20^o = 1.738kN$

Vertical loading
The shaft is loaded vertically as shown in Figure 5

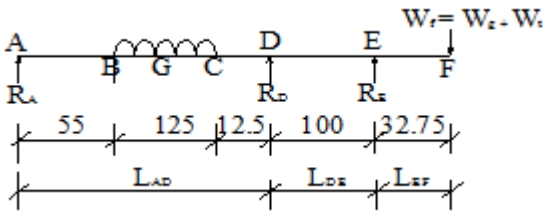


Figure 5: Vertical loading of shaft

This is a statically indeterminate case A, D and E are supports. All of these supports are on the same level

The uniformly distributed load of the screw form is found as

$$w_s = \frac{w_s}{h_{bc}} \qquad (in\ kg/m) \tag{8}$$

$$w_s = \ell_s v_s g \tag{9}$$

A circular section shaft was used to form the screw as such:

$$w_s = \ell_s \frac{H d_s^2}{4} l_s g \tag{10}$$

$$w_s = \frac{(7849.016)(\pi)(8\times10^{-3})^2(277\times10^{-3})(9.81)}{4\times125\times10^{-3}} = 8.577kg/m$$

$$w_s = w_s . l_{bc} \tag{11}$$

$$w_s = (8.577)(0.125) = 1.072Kg$$

The weight of the driven gear mounted on the shaft, $w_g$

$$w_g = \ell v g \tag{12}$$

$$w_g = \ell_s \frac{H d_g^2}{4} l_s g \tag{13}$$

$$w_g = \frac{(7849.016)(\pi)(25\times10^{-3})(16\times10^{-3})(9.81)}{4} = 0.624\text{N}$$

$$w_f \pm w_g + w_t = 0.624 + (4.775\times10^{-3})$$

$$w_f = 4{,}775.624N$$

A solution can be obtained by employing an extension for the moment area method.

Applying clapeyron's equation [6]

$$M_A L_{AD} + 2M_D(L_{AD} + L_{DE}) + M_E L_{DE} = 6\left(\frac{A_{AD}\overline{X_{AD}}}{L_{AD}} + \frac{A_{DE}\overline{X_{DE}}}{L_{DE}}\right) \tag{14}$$

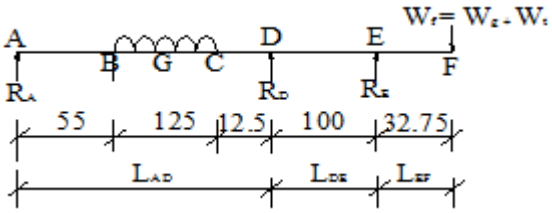


Figure 6: Centroid of bending moment areas

Since A is a support (Figure 3), it follows that

$$M_A = 0$$

$$M_E = W_F x L_{EF}$$

$$= 4775.624 \text{ x } 32.75 \text{ x } 10^{-3}$$

$$M_E = 156.40Nm$$

A sketch of the bending moment areas is shown in Figure 7.

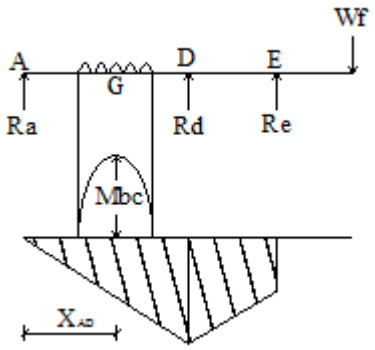


Figure 7: Bending moment areas

The maximum bending moment between span BC is found as

$$M_{BC} = \frac{w_s l_{BC}}{8} \tag{15}$$

$$M_{BC} = \frac{8.577x(125x10^{-3})^2}{8} = 0.0168Nm$$

There is no loading between span $\overline{DE}$ . As such, no free moment area obtains for the span.

$$A_{DE}\overline{X}_{DE} = 0$$

$$\overline{X}_{AD} = \left(55 + \frac{125}{2}\right)x10^{-3} = 117.5x10^{-3}m$$

The actual moments at points A, D and E can be found by algebraically summing the free end fixing moment area. Hence, applying Clapeyron's equation,

$$M_A L_{AD} + 2M_D(L_{AD} + L_{DE}) + M_E L_{DE} = 6\left(\frac{A_{AD}\overline{X_{AD}}}{L_{AD}} + \frac{A_{DE}\overline{X_{DE}}}{L_{DE}}\right) \tag{16}$$

$$\overline{X}_{AD} = 117.5x10^{-3}m$$

$$M_A = 0$$

$$M_E = 156.49Nm$$

$$L_{AD} = (55+125+12.5)x10^{-3}$$

$$= 1925x10^{-3}m$$

$$LDE = 100x10^{-3}m$$

From Figure 7,

$$A_{AD} = A_{BC}$$

$A_{BC}$ = Free bending moment is with span BC =Area under the parabola = $\frac{2}{3}$ x Base of parabola x Height of parabola

Base of the parabola = $L_{BC}$

$$= 125x10^{-3}m$$

Height of the parabola = Maximum bending moment between span BC

$$= \quad M_{BC}$$

$$= \quad \frac{W_s(L_{BC})^2}{8} \tag{17}$$

$$= \frac{8.577x(123x10^{-3})^2}{8}$$

$$\text{Hence, } A_{AD} = \frac{2}{3} * (125x10^{-3}) * \left( \frac{8.577x(125*10^{-3})^2}{8} \right)$$

Substituting in equation (14)

$$0(192.5x10^{-3}) + 2M_D(192.5x10^{-3} + 100x10^{-3}) + 156.40(100x10^{-3})$$

$$A_{AD} = \left[ \left\{ \left( \frac{3}{3} \right) (125x10^{-3}) \left( \frac{8.577x(125x10^{-3})^2}{8} \right) (117.5x10^{-3}) \right\} \right] + 0$$

$$0 + 2M_D(292.5x10^{-3}) + 15.64 = 9.842x10^{-4}$$

$$M_D = \frac{9.842x10^{-4} - 15.64}{2x(292.5x10^{-3})}$$

$$M_D = -26.734Nm$$

To obtain the reactions at the support (fig 2 and 3) we sum moments about "D"
For span AD

$$M_D = -R_A * L_{AD} + w_s * L_{BC} * L_{GC}$$

$$L_{GC} = \left( \frac{125}{2} + 12.5 \right) x10^{-3}$$

$$L_{GC} = 75x10^{-3}m$$

$$M_D = -R_A(192.5x10^{-3}) + (8.577x125x10^{-3})(75.10^{-3})$$

Similarly, for span DF

$$M_D = -W_F * L_{DF} + R_E * L_{DE}$$

$$L_{DE} = (100 + 32.75)x10^{-3}$$

$$= 13275x10^{-3}m$$

$$M_D = -4775.624(132.75x10^{-3}) + R_E(100x10^{-3})$$

Substituting for $M_D$ in equation (30b) and (30b)

$$-26.734 = -R_A(192.5x10^{-3}) + (8.577x125x10^{-3})(75.10^{-3})$$

$$R_A = \frac{(8.577x125x10^{-3})(75.10^{-3}) + 26734}{192.5x10^{-3}}$$

$$= 139.3\text{N}$$

And

$$-26.734 = 4775.624(132.75x10^{-3}) + R_E(100x10^{-3})$$

$$= R_E = \frac{4775.624x132.75x10^{-3} - 26.734}{100x10^{-3}}$$

$$R_E = -6606.981N$$

Summing vertical forces

$$R_A + R_D + R_E = W_F$$

$$139.3 + R_D + (-6606.981) = 4775.624$$

$$R_D = 11243.30N$$

The actual loading diagram for the shaft and shear and bending moment diagrams are shown as Figure 8.

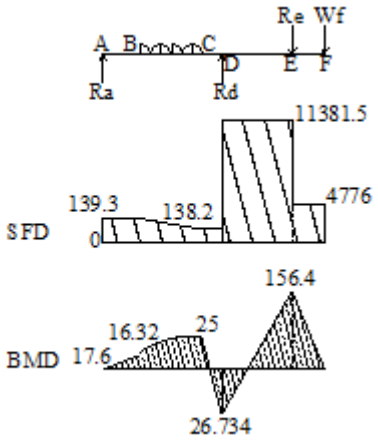


Figure 8: Shear force and bending moment diagram

Shear force analysis

Section A – B

$F = R_A$

$F_A = 139.3N$

Uniform between A and B

Section A – C

At B, F decreases at a rate of = $W_s$, i.e.

$$F = R_A - W_s X$$

At B, x=0 and at C, x = $L_{BC}$

The reduction is greatest at C where:

$$F = R_A - w_s * L_{BC}$$
$$= 139.3 - (8.577x125x10^{-3}$$
$$= 138.22Nm$$

Section A – D (C – D)

F remains uniform at between C and D as $F_C$

Section A – E (D – E)

F is increased by $R_D$ at D

$$F = R_A - w_s * L_{BC} + R_D$$
$$= 139.3 - (8.577x125x10^{-3}) + 11243.3$$
$$F_D = 11381.5N = 11.4KN$$

The value is uniform up to E

Section E – F

At E, F drops by the value $R_E$

$$F = R_A - w_s * L_{BC} + R_D - R_E$$
$$= 139.3 - (8.577x125x10^{-3}) + 11243.3$$
$$F_E = 4776N$$

This is uniform up to F (checked by the value of $W_F$ = 4775.624).

$$M_A = 0$$
$$M_B = R_A.X$$
$$= 139.3x55x10^{-3}$$
$$= 7.662Nm$$
$$M_C = R_A.X - \frac{W_x.L_{BC}}{2}$$
$$L_{AC} = (55+125)x10^{-3}$$
$$= 180x10^{-3}m$$
$$M_C = (139.3x180x10^{-3}) - \frac{8.577x(125x10^{-3})_2}{2}$$
$$= 25.01Nm$$
$$M_G = R_A.X - \frac{W_S L_{BG}^2}{2} = R_A.L_{AG} - \frac{W_S L_{BG}^2}{2}$$
Where $L_{AG} = \left[55 + \left(\frac{125}{2}\right)\right]X10^{-3} = 117.5X10^{-3}$
$$M_G = (139.3X117.5X10^{-3}) - \frac{8.577x162.5x10^{-3})^2}{2}$$
$$M_G = 16.32Nm$$

Horizontal loading

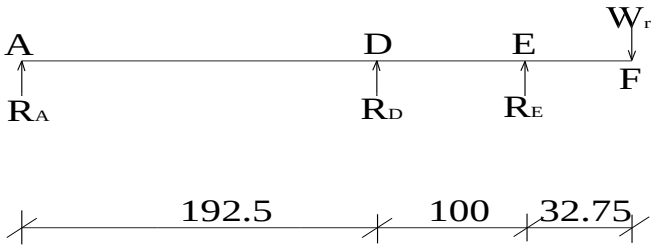


Figure 9: Horizontal loading diagram

$W_r$ = 1738Nm, as determined in preceding paragraphs

The beam is continuous

$$M_A = 0$$
$$M_E = W_r x32.75x10^{-3} = 56.92Nm$$

Applying Clapeyron's equation

$$M_A L_{AD} + 2M_D(L_{AD} + L_{DE}) + M_E L_{DE} = 6\left(\frac{A_{AD}\overline{X}_{AD}}{L_{AD}} + \frac{A_{DE}\overline{X}_{DE}}{L_{DE}}\right) \quad (18)$$
$$0 + 2M_D(292.5x10^{-3}) + (110.365)(100x10^{-3})$$
$$= 6(0+0)$$
$$M_D = \frac{56.92*100x10^{-3}}{2*292.5*10^{-3}}$$
$$M_D = 9.73Nm$$

To find reactions at supports, take moment about C for span AD

$$M_D = -R_A^I * L_{AD}$$
$$R_A^I = \frac{M_D}{L_{AD}} = \frac{9.73}{192.5*10^{-3}} = -50.5N$$

For span DF

$$M_D = R_D^1 * L_{DE} - W_r * L_{DF}$$

$$R_D^1 = \frac{M_D + W_r * L_{DF}}{L_{DE}}$$

$$= \frac{(9.73) + (1738x132.75x10^{-3})}{100x10^{-3}}$$

$$R_D^1 = 2404.5N \text{ and}$$

$$R_A^1 + R_D^1 + R_E^1 = w_r$$

$$\therefore R_A^1 = 1738 - (-50.5) - 2404.5$$

$$\therefore R_A^1 = -2176.0N$$

The bending moment diagram is shown in Figure 10

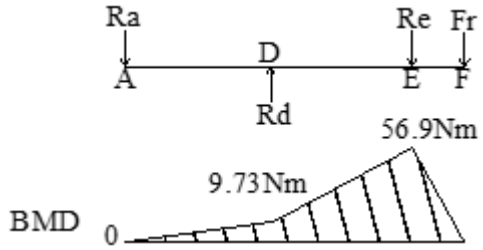


Figure 10: Maximum bending moment

The maximum bending moment on the main shaft obtains at point E and is found as

$$M_{b(\max)} = \sqrt{M_{EH}^2 + M_{EV}^2} \quad (19)$$

Where:

$M_{EV}$ = Vertical B.M. at E

$M_{EH}$ = Horizontal B.M. at E

$$= \sqrt{56.92^2 + 156.4^2}$$

$$M_{b(\max)} = 166.059Nm$$

Maximum torque imposed on this shaft is found from equation (4);

$$M_t = \frac{(9550)(Power)kw}{n} = \frac{(9550)(1.8)}{300} = 57.3Nm$$

The following shock and fatigue factors for bending and torsion were selected for $K_b$ = 1.0, $K_t$ = 1.0 for solid shafts under bending and torsion, with little or no axial loads [5, 6, 7, 8] the ASME code states that

$$d^3 = \frac{16}{\pi b_s}\left[(k_b M_b)^2 + (K_t M_t)^2\right]^{1/2} \quad (20)$$

$$d = \left[\frac{16}{(\pi)(40x10^6)}\left[(1.0)(166.1)^2\right]^2 + \left[1.0x57.3\right]^2\right]^{1/2}\Bigg]^{1/3}$$

$$d = 0.028m$$

**2.3 Hopper Design**

The angle of repose of the product (tomatoes) on stainless steel is 35$^o$ [4] Angle of inclination of the frontal and side faces of the loading bay were selected to be greater than the product angle of repose and are both 37$^o$, this permits complete product evacuation into the feed throat.

**2.3.1 Hopper capacity**

The hopper consists of a loading bay and a feed throat. The shape of the loading bay is that of a truncated right rectangular pyramid (a) while the feed throat is of truncated rectangular prism (b). The volume (Vtp) of the truncated pyramid is obtained using the formula [3]

$$V_{tp} = \left(\frac{h_2 B_2 - h_1 B_1}{3}\right) \quad (21)$$

$V_{tp}$ = $[(198.6*10^{-3})(205*10^{-3})(225*10^{-3}) - (48.6*10^{-3})(50*10^{-3})(75*10^{-3})] / 3$

$= 2.9466*10^{-3}m^3$

$B_2 = l_2 b_2, l_2 = 225 \times 10^{-3}m, b_2 = 205 \times 10^{-3}m, h_2 = 198.6 \times 10^{-3}m, h_1 = 48.6 \times 10^{-3}m$

Volume of the truncated rectangular prism, $V_b$ is given as:

$$V_b = A_b \times h_b \quad (22)$$

$$V_b = A_b \times h_b \quad (23)$$

$A_b = L_b \times W_b, L_b = 75 \times 10^{-3}m, W_b = 50 \times 10^{-3}m, h_b = 75 \times 10^{-3}$

$V_b = (75*50*75)* 10^{-9}m^3$

$= 0.0002813m^3$

$= 0.2813*10^{-3}m^3$

The capacity of the fully loaded hopper, $C_h(kg)$ [8] is:

$$C_h = \gamma_p \times V_h$$

$= 642\ kg/m^3$

Hopper capacity therefore is:

$= (640)\ kg/m^3 * (3.2279*10^{-3})m^3$

$C_h = 2.07kg$

## 2.4. Parts and Assembly Drawings

The pictorial view of the grinding machine is shown in Figure 11. The various parts and assembly drawings of the machine are shown in the appendix.

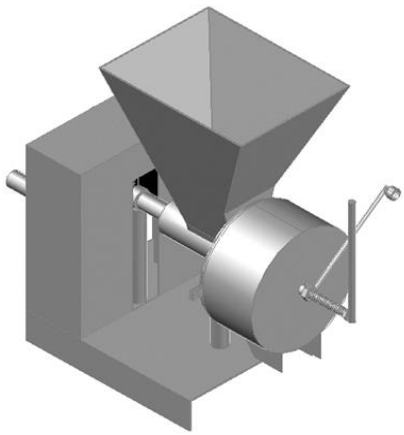

Figure 11: Pictorial View of the Grinding Machine (Isometric)

## 2.5 Cost Analysis

The total costs associated with the machine are grouped into: material cost and fabrication cost and are presented in Table 3 and Table 4 respectively in the appendix section. The summation of the costs gave thirty three thousand and ninety naira (₦ 33, 090.00) only to produce an assembled unit of the manually operated domestic food grinder. This is quite less expensive compared to the conventional grinders used at the markets which costs forty five thousand naira.

## 2.6 Performance Test

Performance test was carried out on both the constructed manually-operated grinder and existing ones with prime mover using fresh tomatoes, pepper, maize, water, 500µm sieve, the constructed machine, existing grinder, bow, measurement scale, and operators.

The following procedures were used for the performance test:

(i) Grind a given amount (500g) of tomatoes, pepper, and maize separately using known quantities of water.

(ii) Measure out 250g of the ground paste and dilute with a litre of water and mix thoroughly;

(iii) Sieve the mixture in (ii) through a 500µm sieve;

(iv) Dry the residue in an oven at a temperature of 105$^{o}$C for 1hour;

(v) Measure the mass of residue;

(vi) Repeat above procedures for each sample ground and take the average residue mass;

(vii) Repeat steps (i) through (vi) above for each type of foodstuff;

(viii) Repeat step (vii) for the existing commercial grinder

## 3. Results and Discussion

The results obtained from the performance tests for the constructed manually operated Grinder are shown in Table 1 while for the convectional Grinder with Prime mover are shown in Table 2:

Table 1: Test Result with the constructed manually operated Grinder

| S/N | PRODUCT | TEST NO. | MASS OF GROUND PASTE MEASURED (Xg) | MASS OF RESIDUE AT 105$^{o}$C | AVERAGE MASS OF RESIDUE (Yg) | GROUND PERCENTAGE $\left(\frac{X-Y}{X}\right) * 100\%$ |
|---|---|---|---|---|---|---|
| 1 | Tomatoes | 1 | 250 | 50 | 47.5 | 81 |
| | | 2 | 250 | 45 | | |
| 2 | Pepper | 1 | 250 | 65 | 63 | 75 |
| | | 2 | 250 | 61 | | |
| 3 | Maize | 1 | 250 | 80 | 81 | 68 |
| | | 2 | 250 | 82 | | |

Table 2: Test Results with the conventional market Grinder

| S/N | PRODUCT | TEST NO. | MASS OF GROUND PASTE MEASURED (Xg) | MASS OF RESIDUE AT 105$^{o}$C | AVERAGE MASS OF RESIDUE (Yg) | GROUND PERCENTAGE $\left(\frac{X-Y}{X}\right) * 100\%$ |
|---|---|---|---|---|---|---|
| 1 | Tomatoes | 1 | 250 | 43 | 45 | 82 |
| | | 2 | 250 | 47 | | |
| 2 | Pepper | 1 | 250 | 58 | 56 | 78 |
| | | 2 | 250 | 54 | | |
| 3 | Maize | 1 | 250 | 68 | 67 | 73 |
| | | 2 | 250 | 66 | | |

Tables 1 and Table 2 shows the performance test results obtained by using the fabricated grinder and the conventional grinder found in our market places respectively. When sample of tomatoes, Pepper and Maize pastes from the constructed machine were evaluated for finness, 81 percent of the Tomatoes had finness of less than 500µm particle size as compared to 82 percent from an existing machine. For Pepper, 75% had finness of less than 500µm particle size as compared to 78 percent from an existing machine and lastly for Maize, 68% had finness of less than 500µm particle size as compared to 73 percent from the conventional machine as can be seen from Table1 and Table 2.

The mass of residue from the constructed machine after drying range from 47.5g to 81g with an average of 63g as can be seen in Table 1 while that from the existing one range from 45g to 67g with an average of 56g. However, in terms of finness of less than 500µm particle size, the overall percentage of the constructed machine was 75% as against 78% for the existing one.

However, the performance of the newly constructed grinder is slightly lower than the conventional existing grinder at the markets but is highly recommended due to its lower cost of purchase and operation. The newly designed machine do not require the use of fuel or electricity and yet give a very close performance to the conventional machines. it is also easy to operate

## 4. Conclusion

The aim of this project was to design and fabricate a manually operated domestic foodstuff grinding machine whose cost is affordable to the common man while ensuring durability, maintainability and reliability are maintained. Hence, it can be concluded that after the design, fabrication and testing of the machine, the results showed an average mass of residue from the constructed machine after drying to be 63g and with a finness of less than 500µm particle size, the overall percentage of the constructed machine was 75percent.

## 5. Conflict of Interest

There is no conflict of interest associated with this work.

## Nomenclatures

| | |
|---|---|
| W | Angular velocity in rad/sec |
| N | rotational speed at the main shaft in rpm |
| H | Trasmitted power in Kwh |
| $M_t$ | Transmitted torque, (Nm) |
| $R_A$, $R_D$ and $R_E$ | Reactions at points A, D and E respectively. |
| Wr | Radial loads on gear tooth. |
| Wg | Weight of the gear mounted on the main shaft. |
| Wt | Tangential load on the gear tooth |
| D | Gear diameter (in mm). |
| $\phi$ | Pressure angle for the gear tooth |
| $w_s$ | Weight of material of the screw (in N), |
| $\ell_{s\,\backslash}$ | Density of screw material (in kg/m$^3$), |
| $d_s$ | Diameter of screw material (in m), |
| $l_s$ | Length of screw material (in m), |
| g | Gravity (in m/s$^2$) |
| $l_{bc}$ | Span $b\bar{c}$ within which the screw is formed (in m). |
| $d_g$ | Diameter of the gear (in m) |
| b | Width of the gear tooth (in m), |

| | |
|---|---|
| $M_A, M_D$ and $M_E$ | Bending moments at supports A, D and E respectively, |
| $S_s$ | Alowable shear stress (in MPa), |
| $M_b$ | Maximum bending moment (in Nm) |
| $M_t$ | Maximum imposed torgue, (in Nm). |
| $B_2$ | Base area of full pyramid, ($m^2$), |
| $l_2$ | Length of the top edge of the loading bay |
| $b_2$ | Width of the top edge of the loading bay, |
| $B_1$ | Base area of bottom edge of the loading bay, ($m^2$), |
| $h_1$ and $h_2$ | Perpendicular height from apex to the top and bottom plane of the loading bay respectively. |
| $A_b$ | Base area of the rectangle, ($m^2$), |
| $L_b$ | Length of the feed throat, (m), |
| $W_b$ | Width of the side face of the feed throat, (m), |
| $h_b$ | Depth of the feed throat, (m). |
| $\gamma_p$ | Product bulk density, $kg/m^3$ |
| $V_h$ | Volume of hopper, $m^3$ |

## References

[1] Ibhadode, A.O. (2001), Introduction to Manufacturing Technology, Ambik Press Publishers, Benin City, pp 62, 427, 445
[2] Healy, B. J., J. D. Hancock, G. A. Kennedy, P. J. Bramel-Cox, K. C. Behnke, and R. H. Hines. (1994). Optimum particle size of corn and hard and soft sorghum for nursery pigs. J. Animal Science. 72: pp22-27
[3] Adetunji O. R. and Quadri A. H. (2011), Design and Fabrication of an Improved Cassava Grater, The Pacific Journal of Science and Technology 12 (2): pp120-129
[4] Wondra, K. J., J. D. Hancock, G. A. Kennedy, R. H. Hines, and K. C. Behnke. (1995). Reducing particle size of corn in lactation diets from 1,200 to 400 micrometers improves sows and litter performance. J. Anim. Sci. 73: pp421-429
[5] Hall, A.S, Holowenko, Laughlin, H.G. (2002). Theory and problems of Machine Design, Schaum's outline series. SI (Metric) Edition, Tata McGraw Hill, New Delhi.
[6] Khurmi, R.S. and Gupta, J.K. (2005), A Textbook of Machine Design (SI units), Eurasia Publishing House (PVT.) Limited, New Delhi, pp 470 – 477, 509 – 515, 996 – 1018, 1101 – 1122.
[7] Robert, H. Creamer (1976). Machine Design, 2nd Edition, Addison- Wesley Series in Engineering Technology. Pp 204 -280, 320-327
[8] Shigley, J.E, Misekhe, C.R, Budynas, R.G, and Nisbett, K.L. (2008). Mechanical Engineering Design, 8th ed, Tata McGraw Hill, New Delhi.

## Appendix A

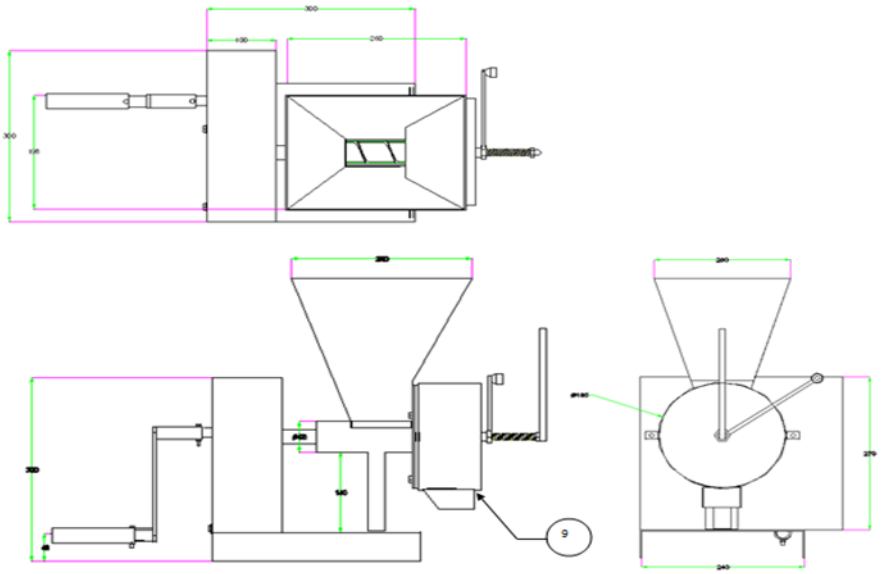

Figure A1: Orthographic Projection of the Grinding Machine

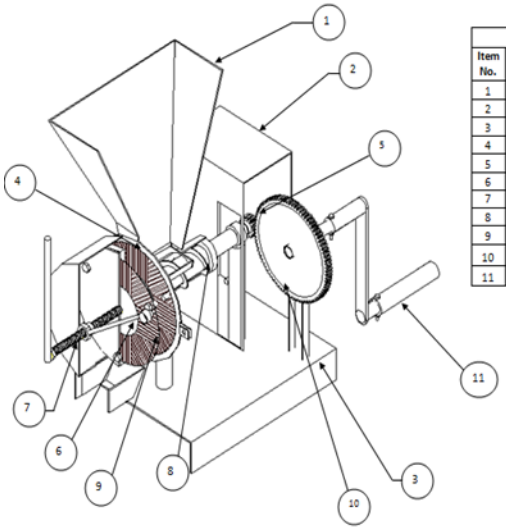


| PARTS LIST | | |
|---|---|---|
| Item No. | Item Description | No. Off |
| 1 | Hopper | 1 |
| 2 | Gear Assembly Guide | 1 |
| 3 | Base | 1 |
| 4 | Grinding Disc Cover | 1 |
| 5 | Pinion | 1 |
| 6 | Locking Nut | 1 |
| 7 | Adjusting Screw | 1 |
| 8 | Shaft | 1 |
| 9 | Grinding Disc | 2 |
| 10 | Gear (Spur) | 1 |
| 11 | Turning Handle | 1 |

Figure A2: Cut-away view of the grinding Machine

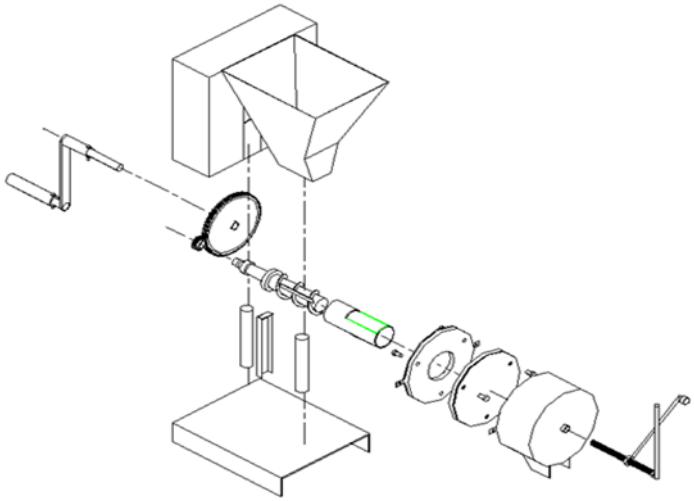

Figure A3: Exploded View of the Grinding Machine

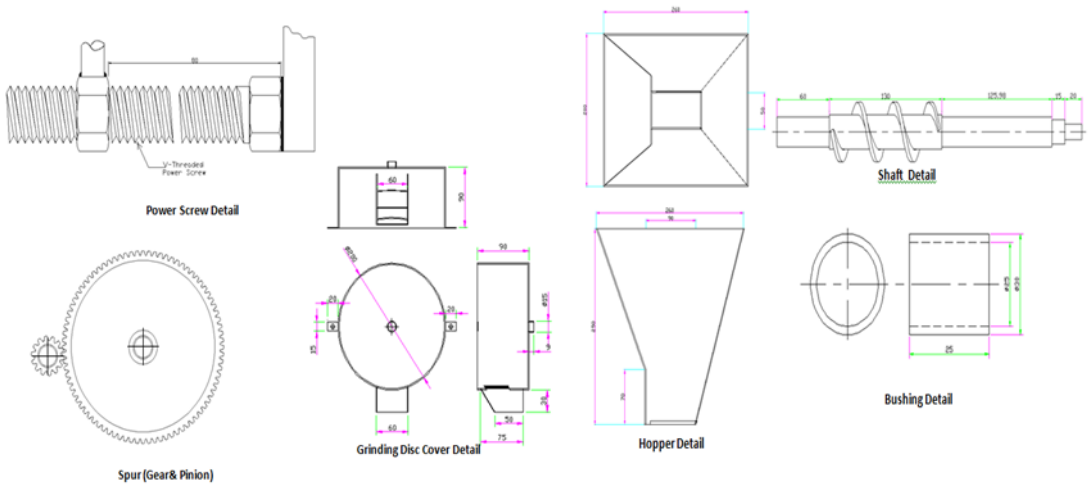


Figure A4: Part Drawing

Figure A5: Final manufactured form of the grinding machine

**Table A1: Material Cost**

| S/N | DESCRIPTION | QTY | AMOUNT (₦) |
|---|---|---|---|
| 1 | 500 * 1000 * 2 mm Stainless Steel Sheet | 1 | 4,500 |
| 2 | 300 * 500 * 6 mm Stainless Steel Plate | 1 | 3,500 |
| 3 | ø 65 * 160 mm Stainless Steel Pipe | 1 | 1,500 |
| 4 | ø 25 * 300 mm Stainless Steel Pipe | 1 | 150 |
| 5 | M6 * 20 mm grub screw | 1 | 100 |
| 6 | M8 * 40 mm Stainless Steel Bolt & Nut | 3 | 240 |
| 7 | M8 * 30 mm C. SK Bolt & Nut | 6 | 600 |
| 8 | 400 * 450 * 1.5 mm M/S Sheet | 1 | 750 |
| 9 | 140 * 60 mm U-Channel ( base) | 1 | 350 |
| 10 | S.W.G. 12 SS Electrode | 20 | 2,000 |
| 11 | Spur Gear (driven) | 1 | 1,500 |
| 12 | Spur Gear (driver) | 1 | 2,500 |
| 13 | Lotus Grinding Disc | 2 | 3,000 |
| 14 | Paint | 2 | 1,400 |
| 15 | 6205 Bearing | 1 | 500 |
| | TOTAL | | 22,590 |

**Table A2: Fabrication Cost**

| S/N | OPERATION | COST (₦) |
|---|---|---|
| 1 | Welding | 3,000 |
| 2 | Machining | 3,000 |
| 3 | Transportation | 3,000 |
| 4 | Miscellaneous | 1,500 |
| TOTAL | | 10,500.00 |